Reactions of $Pt_3Ru_6(CO)_{21}(\mu_3\text{-}H)(\mu\text{-}H)_3$ with Phosphanes – The Synthesis and Structural Characterizations of $[Pt(PMe_3)_3H][Pt_3Ru_6(CO)_{21}(\mu_3\text{-}H)(\mu\text{-}H)_2]$ and $[Pt_3Ru_6(CO)_{20}(PPh_3)(\mu\text{-}H)_3(\mu_3\text{-}H)]$

Richard D. Adams*, Thomas S. Barnard, Zhaoyang Li, and Lijuan Zhang

Department of Chemistry and Biochemistry, University of South Carolina,
29208 Columbia, SC, USA
Fax: (internat.) +1-803/777-6781
E-mail: Adams@psc.sc.edu

Received December 15, 1996

Keywords: Platinum / Ruthenium / Cluster anions / Phosphanes

The reactions of $[Pt_3Ru_6(CO)_{21}(\mu\text{-}H)_3(\mu_3\text{-}H)]$ (**1**) with PMe_3 and PPh_3 have produced the salts $[Pt(PR_3)_3H][Pt_3Ru_6(CO)_{21}(\mu_3\text{-}H)(\mu\text{-}H)_2]$, **5a** and **5d**, R = Me and Ph in the yields 9% and 22%, respectively. By contrast the reaction of **1** with PPh_3 in the presence of Me_3NO has yielded the phosphane-substituted derivative $[Pt_3Ru_6(CO)_{20}(PPh_3)(\mu\text{-}H)_3(\mu_3\text{-}H)]$ (**6**) in 22% yield. Compounds **5a** and **6** were characterized by single crystal X-ray diffraction analysis. Compounds **5a** and **5d** are salts of the anion $[Pt_3Ru_6(CO)_{21}(\mu_3\text{-}H)(\mu\text{-}H)_2]^-$. The anion contains a layer segregated $Ru_3Pt_3Ru_3$ structure similar to that of **1** with two bridging hydride ligands on one Ru_3 triangle and one semi-triply bridging hydride ligand on the other. The cation $[Pt(PR_3)_3H]^+$ was evidently formed by the abstraction of platinum from other molecules of **1**. Compound **6** is a PPh_3 derivative of the parent **1** that also contains the layer segregated stacking of Ru_3 and Pt_3 triangles. The PPh_3 ligand is coordinated to one of the ruthenium atoms in an axial position.

Introduction

Mixed metal cluster complexes are of interest because of their potential of cooperative reactivity and "synergism" in their transformations of small organic molecules and in catalysis[1]. We have recently prepared a series of mixed metal cluster complexes that contain the first examples of layer segregated triangular stacks of platinum combined with ruthenium[2,3] or osmium[4]. The platinum-ruthenium complex $Pt_3Ru_6(CO)_{21}(\mu\text{-}H)_3(\mu_3\text{-}H)$ (**1**) has been shown to react with diphenylacetylene to yield the derivative $Pt_3Ru_6(CO)_{20}(\mu\text{-}PhC_2Ph)(\mu\text{-}H)(\mu_3\text{-}H)$ (**2**) in which the diphenylacetylene ligand is found to be coordinated as a triple bridge to one of the triruthenium triangles[2]. Interestingly, **2** serves as an active catalyst for the hydrogenation of diphenylacetylene to *Z*-stilbene compared to other cluster complexes. This has been attributed to synergistic effects involving the different types of metal atoms[5].

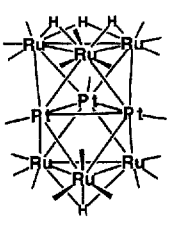

1

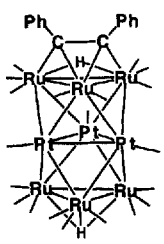

2

We have shown that **1** is deprotonated by base (OH^-) and the resultant anions can be used to prepare a variety of the mixed metal cluster complexes: $Pt_3Ru_6[Au(PEt_3)](CO)_{21}(\mu\text{-}H)_3$ (**3**)[6], $Pt_3Ru_6[Au(PEt_3)]_2(CO)_{21}(\mu_3\text{-}H)_2$ (**4**)[6], $Pt_3Ru_6(CO)_{21}(\mu_3\text{-IrCp*})(\mu_3\text{-}H)_2$[7], and $[NBu_4][Pt_3Ru_6(CO)_{21}(\mu_3\text{-HgI})(\mu_3\text{-}H)_2]$[7].

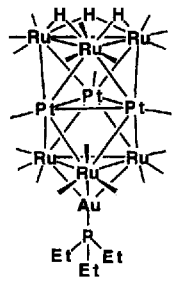

3

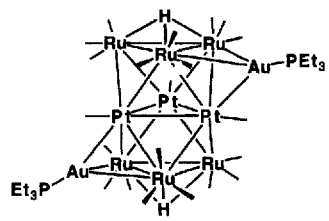

4

In order to understand the site reactivity of this unusual class of mixed metal cluster complexes further, we have investigated the reactions of **1** with selected phosphanes in the presence and absence of the CO activation agent Me_3NO. These results are reported here.

Results

The reaction of **1** with the phosphanes PMe_3 and PPh_3 at room temperature yielded the compounds $[Pt(PR_3)_3H][Pt_3Ru_6(CO)_{21}(\mu_3\text{-}H)(\mu\text{-}H)_2]$, **5a** and **5d**, R = Me and Ph in 9% and 22% yield, respectively after workup by TLC. Compounds **5a** and **5d** are salts of the anion $[Pt_3Ru_6(CO)_{21}(\mu_3\text{-}H)(\mu\text{-}H)_2]^-$[6]. Two minor products **5b** and **5c** were also obtained from the reaction that yielded **5a**. The infrared spectrum of these compounds in the CO region was virtually the same as that of **5a** indicating that they also salts of the anion $[Pt_3Ru_6(CO)_{21}(\mu_3\text{-}H)(\mu\text{-}H)_2]^-$,

  0009–2940/97/0606–0729 $ 17.50+.50/0

but due to the small amounts of material, the identity of the counter ion could not be established.

Compound **5a** was characterized crystallographically. An ORTEP diagram of the structure of the anion $[Pt_3Ru_6(CO)_{21}(\mu_3\text{-}H)(\mu\text{-}H)_2]^-$ is shown in Figure 1. Selected bond distances are given in Table 1. The anion is structurally very similar to that of **1**. It contains a $Ru_3Pt_3Ru_3$ cluster stacked in triangular layers in staggered conformations. There are two hydride ligands bridging two edges of one of the Ru_3 triangles and one semi-triply bridging hydride ligand on the other Ru_3 triangle. In **1** there are three edge bridging hydride ligands on one Ru_3 triangle and one triply bridging hydride on the other[2]. As expected, the Ru–Ru bond distances in **5a** that contain the edge bridging hydride ligands are significantly longer than the one that does not, Ru(1)–Ru(2) = 2.978(4) Å and Ru(1)–Ru(3) = 3.052(4) Å vs. Ru(2)–Ru(3) = 2.856(3) Å. The hydride-bridged Ru–Ru distances in **1** have similar lengths[2]. The other hydride ligand H(1) appears to be a semitriple bridge, Ru(4)–H(1) = 2.59 Å vs. Ru(5)–H(1) = 2.00 Å and Ru(6)–H(1) = 1.59 Å. Curiously, it seems to be most strongly associated with the shortest of the three Ru–Ru bonds, Ru(5)–Ru(6) = 2.947(4) Å. Despite this result, the splaying out of the two carbonyl ligands C(51)–O(51) and C(62)–O(62), as indicated by the large bond angles Ru(6)–Ru(5)–C(51) = 125.0(8)° and Ru(5)–Ru(6)–C(62) = 114(1)° also indicates that the hydride ligand does bridge the Ru(5)–Ru(6) bond as shown in Figure 1. As in **1** and **3**, the Pt_3 triangle does not lie midway between the two Ru_3 triangles, but lies closest to the Ru_3 triangle containing the semitriply bridging hydride ligand [Pt_3–Ru_3(456) = 2.20 Å vs. Pt_3–Ru_3(123) = 2.33 Å]. Each ruthenium atom contains three carbonyl ligands and each platinum atom has one. All are terminal CO ligands except C(61)–O(61) which is a strong semi-bridge from Ru(6) to Pt(2), Ru(6)–C(61) = 1.93(4) Å, Pt(2)–C(61) = 2.44(3) Å and Ru(6)–C(61)–O(61) = 152(3)°.

Figure 1. An ORTEP diagram of the anion $[Pt_3Ru_6(CO)_{21}(\mu\text{-}H)_2(\mu_3\text{-}H)]^-$ (**5a**) showing 40% probability thermal ellipsoids

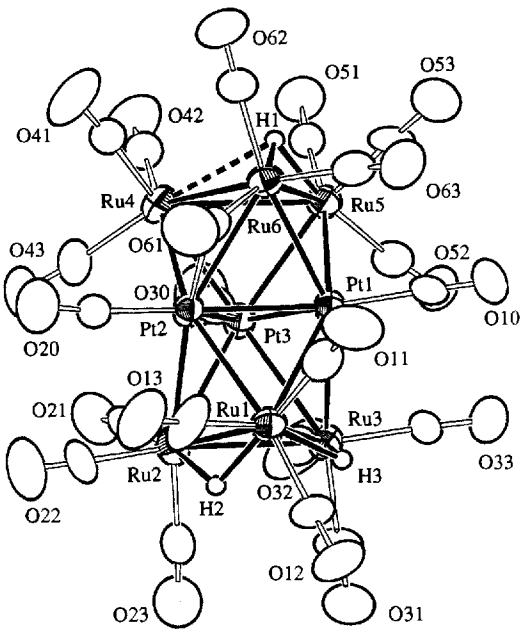

Table 1. Intramolecular distances of **5a** (distances in Å, estimated standard deviations in the least significant figure are given in parentheses)

Atom	Atom	Distance	Atom	Atom	Distance
Pt(1)	Pt(2)	2.633(1)	Ru(2)	C(22)	1.88(3)
Pt(1)	Pt(3)	2.668(2)	Ru(2)	C(23)	1.87(4)
Pt(1)	Ru(1)	2.895(3)	Ru(2)	H(2)	2.12
Pt(1)	Ru(3)	2.822(3)	Ru(3)	C(31)	1.89(3)
Pt(1)	Ru(5)	2.699(2)	Ru(3)	C(32)	2.02(4)
Pt(1)	Ru(6)	2.759(2)	Ru(3)	C(33)	1.86(3)
Pt(1)	C(10)	1.90(3)	Ru(3)	H(3)	1.71
Pt(2)	Pt(3)	2.697(2)	Ru(4)	Ru(5)	3.070(3)
Pt(2)	Ru(1)	2.806(2)	Ru(4)	Ru(6)	2.995(4)
Pt(2)	Ru(2)	2.826(3)	Ru(4)	C(41)	1.94(3)
Pt(2)	Ru(4)	2.740(3)	Ru(4)	C(42)	1.87(3)
Pt(2)	Ru(6)	2.834(3)	Ru(4)	C(43)	1.90(3)
Pt(2)	C(20)	1.87(3)	Ru(4)	H(1)	2.59
Pt(2)	C(61)	2.44(3)	Ru(5)	Ru(6)	2.947(4)
Pt(3)	Ru(2)	2.898(3)	Ru(5)	C(51)	1.91(3)
Pt(3)	Ru(3)	2.849(2)	Ru(5)	C(52)	1.94(3)
Pt(3)	Ru(4)	2.724(2)	Ru(5)	C(53)	1.84(3)
Pt(3)	Ru(5)	2.722(3)	Ru(5)	H(1)	2.00
Pt(3)	C(30)	1.84(4)	Ru(6)	C(61)	1.93(3)
Pt(4)	P(1)	2.30(1)	Ru(6)	C(62)	1.90(3)
Pt(4)	P(2)	2.315(9)	Ru(6)	C(63)	1.93(4)
Pt(4)	P(3)	2.29(1)	Ru(6)	H(1)	1.56
Pt(4)	H(4)	1.9(2)	P(1)	C(101)	1.75(4)
Ru(1)	Ru(2)	2.978(4)	P(1)	C(102)	1.78(4)
Ru(1)	Ru(3)	3.052(4)	P(1)	C(103)	1.81(4)
Ru(1)	C(11)	1.91(4)	P(2)	C(201)	1.76(4)
Ru(1)	C(12)	1.93(3)	P(2)	C(202)	1.75(3)
Ru(1)	C(13)	1.90(3)	P(2)	C(203)	1.80(4)
Ru(1)	H(2)	1.57	P(3)	C(301)	1.82(4)
Ru(1)	H(3)	1.90	P(3)	C(302)	1.81(4)
Ru(2)	Ru(3)	2.856(3)	P(3)	C(303)	1.80(3)
Ru(2)	C(21)	1.92(4)	O	C(av)	1.14(3)

The hydride ligands on the cluster exhibit a single resonance at $\delta = -16.94$ at 25 °C which is indicative of an averaging process which was also observed in **1**. Upon cooling to −90 °C, this resonance reforms as two resonances in a 2:1 ratio, $\delta = -16.05$ (2H) and −19.50 (1H). An ORTEP diagram of the structure of the $[Pt(PMe_3)_3H]^+$ cation is shown in Figure 2. It is structurally and spectroscopically indistinguishable from its formula equivalent as previously characterized in the form of the salt $[Pt(PMe_3)_3H][BPh_4]$[8]. It possesses a distorted square planar structure. The position of the hydride ligand was located and refined, $\delta = -5.78$ (dt, 1H, Pt-H, $^2J_{P\text{-}H(trans)} = 168.2$ Hz, $^2J_{P\text{-}H(cis)} = 19.2$ Hz, $^1J_{Pt\text{-}H} = 856.6$ Hz).

When PMe_3 was added to a solution of **1** in an NMR tube in $CDCl_3$ solvent, the resonances of the cluster anion formed promptly. However, the resonances of the anticipated cation $[Pt(PMe_3)_3H]^+$ could not be confirmed.

Compound **5d** is spectroscopically similar to **5a** except for the known differences in the ^{1}H-NMR pattern of the $[Pt(PPh_3)_3H]^+$ cation[9]. Compound **5d** is therefore believed to be a simple PPh_3 homolog of **5a**.

When **1** was allowed to react with PPh_3 in the presence of one equivalent of the CO activation agent Me_3NO, the

Figure 2. An ORTEP diagram of the cation $[Pt(PMe_3)_3H]^+$ of **5a** showing 40% probability thermal ellipsoids

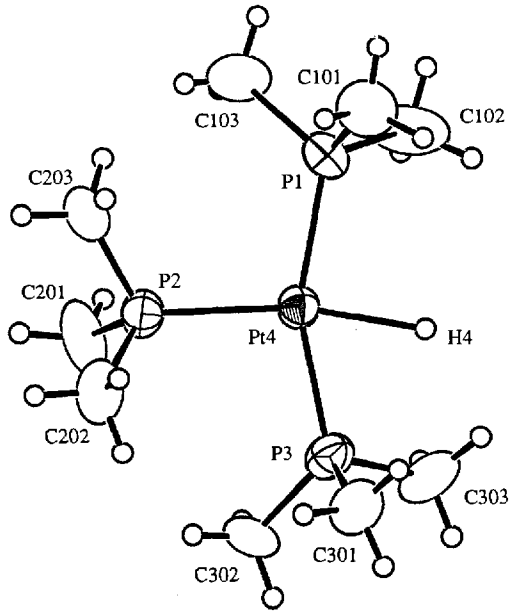

Figure 3. An ORTEP diagram of $[Pt_3Ru_6(CO)_{20}(PPh_3)(\mu\text{-}H)_3(\mu_3\text{-}H)]$ (**6**) showing 40% probability thermal ellipsoids

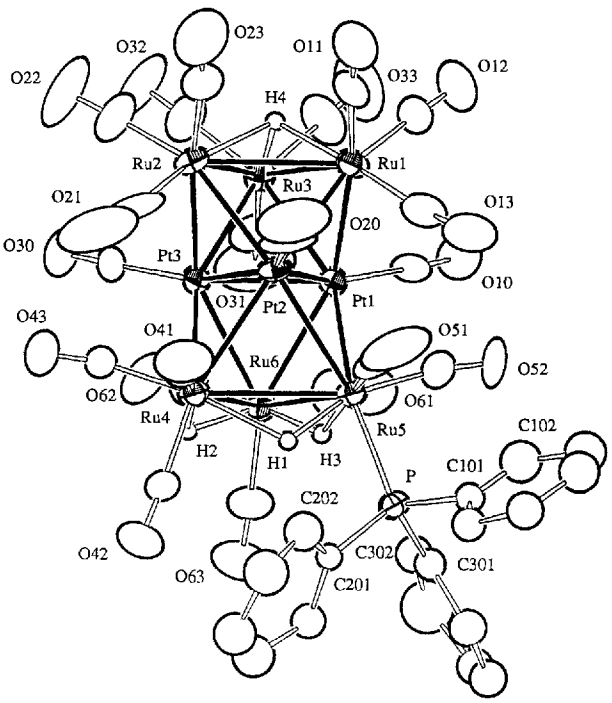

phosphane substituted derivative $[Pt_3Ru_6(CO)_{20}(PPh_3)(\mu\text{-}H)_3(\mu_3\text{-}H)]$ (**6**) was obtained in 22% yield. Compound **6** was characterized by single crystal X-ray diffraction analysis. An ORTEP diagram of the molecular structure of **6** is shown in Figure 3. Selected bond distances are given in Table 2. Compound **6** is a PPh_3 derivative of the parent **1** that contains a similar stacking of Ru_3 and Pt_3 triangular metal groups. The PPh_3 ligand is coordinated to one of the ruthenium atoms Ru(5), Ru(5)–P = 2.356(4) Å in an "axial" position, that it is directed away from the Pt_3 layer of the cluster. The four hydride ligands were located and refined in the analysis. As in **1** there are three edge bridging hydride ligands on one Ru_3 triangle, Ru(4)–Ru(5)–Ru(6), and one triply bridging hydride on the other, Ru(1)–Ru(2)–Ru(3). All of the Ru–Ru bond distances are greater than 3.00 Å due to the bond lengthing effect produced by the hydride ligands. As in **1** and **5a** the Pt_3 triangle lies closest to the Ru_3 triangle that contains the triply bridging hydride ligand. The Pt_3 to Ru_3(123) distance is 2.15 Å while the Pt_3-to-Ru_3(456) distance is 2.36 Å. The hydride ligands in **6** are also dynamically active on the NMR timescale. At room temperature no signal is observed for the the hydride ligands in **6** in its ^{1}H-NMR spectrum, however at −90 °C, three resonances are observed, $\delta = -17.04$ (d, 2H, $^2J_{P\text{-}H}$ = 8.3 Hz), −18.37 (s, 1H) and −23.37 (s, 1H) which is consistent with that of the solid state structure.

Table 2. Intramolecular distances of **6** (distances in Å, estimated standard deviations in the least significant figure are given in parentheses)

Atom	Atom	Distance	Atom	Atom	Distance
Pt(1)	Pt(2)	2.6401(8)	Ru(1)	H(4)	1.9(1)
Pt(1)	Pt(3)	2.6269(8)	Ru(2)	Ru(3)	3.030(2)
Pt(1)	Ru(1)	2.697(1)	Ru(2)	H(4)	2.1(1)
Pt(1)	Ru(3)	2.723(1)	Ru(3)	H(4)	2.0(1)
Pt(1)	Ru(5)	2.884(1)	Ru(4)	Ru(5)	3.021(2)
Pt(1)	Ru(6)	2.873(1)	Ru(4)	Ru(6)	3.027(2)
Pt(2)	Pt(3)	2.6227(9)	Ru(4)	H(1)	2.1(1)
Pt(2)	Ru(1)	2.718(1)	Ru(4)	H(2)	1.9(1)
Pt(2)	Ru(2)	2.734(1)	Ru(5)	Ru(6)	3.030(2)
Pt(2)	Ru(4)	2.878(1)	Ru(5)	P	2.356(4)
Pt(2)	Ru(5)	2.882(1)	Ru(5)	H(1)	1.7(1)
Pt(3)	Ru(2)	2.700(1)	Ru(5)	H(3)	1.6(1)
Pt(3)	Ru(3)	2.711(1)	Ru(6)	H(2)	1.8(1)
Pt(3)	Ru(4)	2.893(1)	Ru(6)	H(3)	1.7(1)
Pt(3)	Ru(6)	2.888(1)	Pt	C(av)	1.87(2)
Ru(1)	Ru(2)	3.065(2)	Ru	C(av)	1.89(2)
Ru(1)	Ru(3)	3.040(2)	O	C(av)	1.14(2)

Discussion

The reactions investigated in this study are summarized in Scheme 1. The reaction of **1** with tertiary phosphanes in solution leads to the formation of the monoanion $[Pt_3Ru_6(CO)_{21}(\mu_3\text{-}H)(\mu\text{-}H)_2]^-$ by a deprotonation step. we have shown previously that **1** can be deprotonated by Lewis bases to yield the monoanion $[Pt_3Ru_6(CO)_{21}(\mu_3\text{-}H)(\mu\text{-}H)_2]^-$[6]. The nature of the cation formed in the reaction with PMe_3 could not be confirmed by ^{1}H-NMR spectra of the solutions. In particular, the resonances of the anticipated cations, $[Me_3PH]^+$ and $[Pt(PMe_3)_3H]^+$, were not evident in these solutions. However, after separation by TLC in air the salt **5a** containing the cation $[Pt(PMe_3)_3H]^+$ was clearly present. Accordingly, it is suspected that $[Pt(PMe_3)_3H]^+$ cation was formed by degradation of a portion of the complex in the workup procedure.

When solutions of **1** were treated with a combination of PPh_3 and the CO activation agent Me_3NO[10], then the phosphane substituted derivative of **1**, **6** was obtained. In this case the Me_3NO almost certainly has promoted a CO

elimination process that facilitates the entry of the phosphane ligand into the coordination sphere of the cluster. The Me_3NO reaction may occur preferentially at the carbonyl groups on the ruthenium atom where the phosphane ligand was found in **6** for steric reasons. Me_3NO is known to attack directly at the CO carbon atom[10]. The carbon atoms of the platinum bound carbonyl groups seem to be much less accessible than those on the ruthenium atoms.

Scheme 1

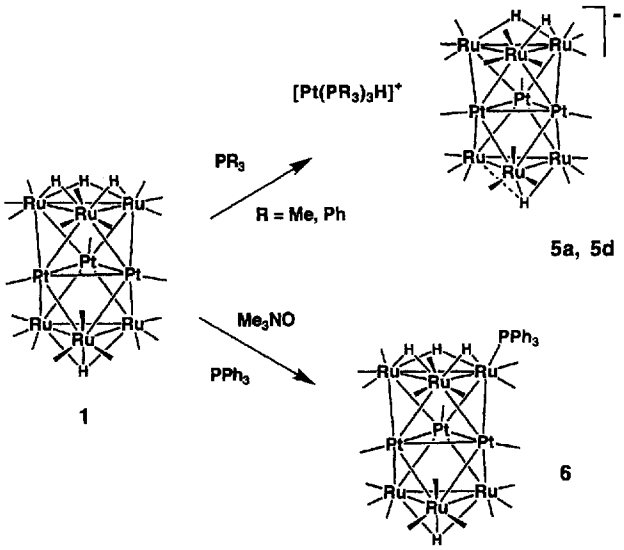

This research was supported by the *National Science Foundation*. We wish to thank Mr. *John Yamamoto* for recording the variable-temperature NMR spectra.

Experimental Section

All reactions were performed under a nitrogen atmosphere unless specified otherwise. Complex **1** was prepared by our previously reported procedure[2]. Dichloromethane was dried and distilled from P_2O_5. NMR solvents were dried over 5 Å molecular sieves. – NMR spectra were run on a Bruker AM-500 spectrometer operating at 500 MHz. – Elemental Analyses were performed by Oneida Research Services Inc., Whitesboro, NY and Desert Analytics, Tucson, AZ. – Chromatographic separations were performed in air on Analtech 0.25 mm silica gel 60 Å F_{254} plates.

Preparation of $[Pt(PMe_3)_3H][Pt_3Ru_6(CO)_{21}(\mu_3\text{-}H)(\mu\text{-}H)_2]$ (**5a**) *and* $[Pt(PPh_3)_3H][Pt_3Ru_6(CO)_{21}(\mu_3\text{-}H)(\mu\text{-}H)_2]$ (**5d**): A 40.0-mg amount of **1** (0.0224 mmol) was dissolved in 60 ml of CH_2Cl_2. A 67.2 µl amount of a 1.0 M toluene solution of PMe_3 (0.0672 mmol) was added to the reaction solution via syringe. The solution was stirred at room temperature for 16 h. The solvent was removed in vacuo and the residue separated by TLC using a hexane/CH_2Cl_2 (1:2) mixture. Several small bands eluted first. These could not be characterized due to the small amounts. These bands were followed by three larger red-brown bands which yielded in order of elution: 4.5 mg of $[Pt(PMe_3)_3H][Pt_3Ru_6(CO)_{21}(\mu_3\text{-}H)(\mu\text{-}H)_2]$, **5a** (9%). 3.6 mg of **5b** and 1.8 mg of **5c**. – Spectral data for **5a**: IR (νCO, in cm^{-1}, in CH_2Cl_2): 2046 (s, sh), 2033 (vs), 2017 (s, sh). – ^1H NMR (δ in CD_2Cl_2): 1.72 (t, 18H, PCH_3, $^2J_{P\text{-}H}$ = 3.7 Hz, $^3J_{Pt\text{-}H}$ = 35.1 Hz), 1.60 (dd, 9H, PCH_3, $^4J_{H\text{-}H}$ = 1.3 Hz, $^2J_{P\text{-}H}$ = 8.7 Hz, $^3J_{Pt\text{-}H}$ = 20.5 Hz), −5.78 (dt, 1H, Pt-H, $^2J_{P\text{-}H(trans)}$ = 168.2 Hz, $^2J_{P\text{-}H(cis)}$ = 19.2 Hz, $^1J_{Pt\text{-}H}$ = 856.6 Hz), −16.94 (s, br., 3H). – ^1H NMR (δ in CD_2Cl_2 at −90 °C): 1.64 (s, br., 18H, PCH_3, $^3J_{Pt\text{-}H}$ = 34.8 Hz), 1.53 (d, br., 9H, PCH_3, $^2J_{P\text{-}H}$ = 8.9 Hz), −5.59 (dt, 1H, Pt-H, $^2J_{P\text{-}H(trans)}$ = 167.0 Hz, $^2J_{P\text{-}H(cis)}$ = 18.7 Hz, $^1J_{Pt\text{-}H}$ = 858.4 Hz), −16.05 (s, 2H), −19.50 (s, 1H). – $C_{30}H_{30}O_{21}P_3Pt_4Ru_6$: calcd. (found) C 16.32 (15.34), H 1.42 (1.35). – The IR spectra of **5b** and **5c** in the CO region is the same as that of **5a**. We were unable to characterize **5b** and **5c** further. – The compound $[Pt(PPh_3)_3H][Pt_3Ru_6(CO)_{21}(\mu_3\text{-}H)(\mu\text{-}H)_2]$, **5d** was prepared in a similar fashion in a 22% yield. – Spectral data for **5d**: IR (νCO, in cm^{-1}, in CH_2Cl_2): 2045 (s, sh), 2033 (vs), 2016 (s, sh). – ^1H NMR at 25 °C (δ in CD_2Cl_2): 7.58–7.01 (m, 45H, Ph), −5.75 (ddd, 1H, Pt-H, $^2J_{P\text{-}H(trans)}$ = 159.8 Hz, $^2J_{P\text{-}H(cis)}$ = 12.9 Hz, $^1J_{Pt\text{-}H}$ = 772 Hz), −16.93 (s, br., 3H).

Preparation of $Pt_3Ru_6(CO)_{20}(PPh_3)(\mu_3\text{-}H)(\mu\text{-}H)_3$ (**6**): A 20.0-mg amount of **1** (0.0112 mmol) and 4.4 mg of PPh_3 (0.0168 mmol) were dissolved in 50 ml of CH_2Cl_2. A 1.0-mg amount of Me_3NO (0.0134 mmol) dissolved in 1 ml CH_2Cl_2 was added to the above solution quickly through a dropping funnel. The resulting solution was stirred at room temperature for 10 min. The solvent was removed in vacuo and the residue separated by TLC using a hexane/CH_2Cl_2 (2:1) mixture. This yielded 5.0 mg of purple-red $Pt_3Ru_6(CO)_{20}PPh_3(\mu_3\text{-}H)(\mu\text{-}H)_3$, **6** (22%). – IR (νCO, in cm^{-1}, in hexane): 2093 (w), 2056 (vs), 2049 (s, sh), 2023 (w). – ^1H NMR (δ in CD_2Cl_2 at −90 °C): 7.52–7.41 (m, 15H, Ph), −17.04 (d, 2H, $^2J_{P\text{-}H}$ = 8.3 Hz), −18.37 (s, 1H), −23.37 (s, 1H). – $C_{38}H_{19}O_{20}P_3Pt_3Ru_6$: calcd. (found) C 22.62 (22.32), H 0.95 (0.94).

Crystallographic Analyses: Crystals of **5a** were grown from a solution in a 1:1 CH_2Cl_2/benzene solvent mixture by slow evaporation of the solvent at 25 °C. Crystals of **6** suitable for X-ray diffraction analysis were grown from a solution in a dichloromethane/hexane (1:1) solvent mixture by slow evaporation of the solvent at 25 °C. The crystals (size: **5a**: 0.5 × 0.5 × 0.02 mm; **6**: 0.45 × 0.15 × 0.04 mm) used in intensity measurements were mounted in thin-walled glass capillaries. Diffraction measurements were made on a Rigaku AFC6S automatic diffractometer by using graphite-monochromated Mo-K_α radiation. The unit cells were determined

Table 3. Crystal data for compounds **5a** and **6**

Compound	**5a**	**6**
Formula	$Pt_4Ru_6P_3O_{21}C_{30}H_{31}$	$Pt_3Ru_6PO_{20}C_{38}H_{19}$
Formula weight	2207.26	2018.22
Crystal system	monoclinic	monoclinic
Lattice parameters		
a [Å]	15.907(2)	10.181(1)
b [Å]	17.632(4)	15.197(2)
c [Å]	19.051(5)	31.249(3)
β [°]	101.56(2)	91.29(1)
V [Å^3]	5235(2)	4834(2)
Space group	$P2_1/n$(#14)	$P2_1/c$(#14)
Z value	4	4
ρ_{calc} [g/cm^3]	2.80	2.77
µ (Mo-*Kα*) [cm^{-1}]	124.4	106.3
T [°C]	20	20
2Θmax [°]	42	42
No. Obs. [$I>3\sigma(I)$]	3897	3863
Goodness of fit (GOF)[a]	2.85	1.40
Residuals[a]: *R*; R_w	0.056; 0.055	0.030; 0.030
Largest peak in final diff. map	2.2	1.16
abs. corr., Max/min	empirical, 1.00/0.057	empirical, 1.00/0.88

[a] $R = \Sigma_{hkl}(||F_{obs}|-|F_{calc}||)/\Sigma_{hkl}|F_{obs}|$; $R_w = [\Sigma_{hkl}w(|F_{obs}|-|F_{calc}|)^2/\Sigma_{hkl}wF_{obs}^2]^{1/2}$, $w = 1/\sigma^2(F_{obs})$; GOF = $[\Sigma_{hkl}w(|F_{obs}|-|F_{calc}|)^2/(n_{data}-n_{vari})]^{1/2}$.

from 25 randomly selected reflections obtained by using the AFC6 automatic search, center, index, and least-squares routines. Crystal data, data collection parameters, and results of the analyses are listed in Table 3. All data processing was performed on a Digital Equipment Corp. VAX station 3520 computer by using the TEXSAN structure solving program library obtained from the Molecular Structure Corp., The Woodlands, TX. Lorentz-polarization (Lp) and absorption corrections were applied to the data in each analysis. Neutral atom scattering factors were calculated by the standard procedures[11a]. Anomalous dispersion corrections were applied to all non-hydrogen atoms[11b]. Both structures were solved by a combination of direct methods (MITHRIL) and difference Fourier syntheses. Full matrix least-squares refinements minimized the function: $\Sigma_{hkl} w(|F_o|-|F_c|)^2$, where $w = 1/\sigma(F)^2$, $\sigma(F) = \sigma(F_o^2)/2F_o$ and $\sigma(F_o^2) = [\sigma(I_{raw})^2 + (0.02\ I_{net})^2]^{1/2}/\mathrm{Lp}$.

Compound **5a** crystallized in the monoclinic crystal system. The space group $P2_1/n$ was established on the basis of the patterns of systematic absences observed in the data. All nonhydrogen atoms were refined with anisotropic thermal parameters. The three hydride ligands on the Pt_3Ru_6 cluster anion were located and partially refined and then fixed in the final cycles of refinement. The hydride ligand H(4) on the $[Pt(PMe_3)_3H]^+$ cation was located and refined to convergence on its positional parameters using a fixed isotropic thermal parameter. The hydrogen atoms on the PMe_3 ligands on the cation were calculated by assuming idealized geometry, C–H = 0.95 Å. Their scattering contributions were added to the structure factor calculations, but their positions were not refined.

Compound **6** crystallized in the monoclinic crystal system. The space group $P2_1/c$ was established on the basis of the patterns of systematic absences observed in the data. The metal and phosphorus atoms and carbon and oxygen atoms of the CO ligands were refined with anisotropic thermal parameters. Each of the phenyl rings of the PPh_3 ligand exhibited a two-fold rotational disorder, thus these atoms were refined with isotropic thermal parameters only. The positions of the four hydride ligands were obtained in difference Fourier syntheses, and they were refined on their positional parameters with fixed thermal parameters, $B = 4.0$. Due to the disorder, the hydrogen atoms on the phenyl rings were omitted.

Further details of the crystal structure investigations are available from the Fachinformationszentrum Karlsruhe, D-76344 Eggenstein-Leopoldshafen (Germany), on quoting the depository number CSD-59391.

[1] P. Braunstein, J. Rosé, in *Comprehensive Organometallic Chemistry*, (Eds.: G. Wilkinson, F. G. A. Stone, E. Abel), 2nd Ed., Pergamon, Oxford, **1995**, vol. 10, ch. 7. pp. 351.

[2] R. D. Adams, T. S. Barnard, Z. Li, W. Wu, J. H. Yamamoto, *Organometallics*, **1994**, *13*, 2357.

[3] R. D. Adams, Z. Li, W. Wu, *Organometallics* **1992**, *11*, 4001.

[4] [4a] R. D. Adams, J.-C. Lii, W. Wu, *Inorg. Chem.* **1991**, *30*, 3613. – [4b] R. D. Adams, J.-C. Lii, W. Wu, *Inorg. Chem.* **1992**, *31*, 2556. – [4c] R. D. Adams, J.-C. Lii, W. Wu, *Inorg. Chem.* **1991**, *30*, 2257.

[5] R. D. Adams, T. S. Barnard, Z. Li, W. Wu, J. H. Yamamoto, *J. Am. Chem. Soc.* **1994**, *116*, 9103.

[6] R. D. Adams, T. S. Barnard, J. E. Cortopassi, *Organometallics* **1995**, *14*, 2232.

[7] R. D. Adams, T. S. Barnard, J. E. Cortopassi, L. Zhang, *Organometallics* **1996**, *15*, 2664.

[8] D. L. Packett, A. Syed, W. C. Trogler, *Organometallics* **1988**, *7*, 159.

[9] [9a] T. W. Dingle, K. R. Dixon, *Inorg. Chem.* **1974**, *13*, 846. – [9b] K. Thomas, J. T. Dumler, B. W. Renoe, C. J. Nyman, D. M. Roundhill, *Inorg. Chem.* **1972**, *11*, 1795.

[10] T. Y. Luh, *Coord. Chem. Rev.* **1984**, *60*, 255.

[11] *International Tables for X-ray Crystallography*, Kynoch Press: Birmingham, England, **1975**; Vol IV: [11a] Table 2.2B, pp. 99–101; [11b] Table 2.3.1, pp. 149–150.

[96271]